Electronic Supplementary Information

Assembling Novel Fast-Acting Pyrazole/Pyridine-Functionalized N-Heterocyclic Carbene Silver Complexes in Nanoparticles Show Enhanced Safety and Efficacy as Anticancer Therapeutics

Chao Chen,[a,b] Liqian Zhou,[a] Binbin Xie,[c] Yuchen Wang,[a] Lulu Ren,[c] Xiaona Chen,[a] Beini Cen,[a] Lv He,[b] and Hangxiang Wang*[a]

[a] *The First Affiliated Hospital; Key Laboratory of Combined Multi-Organ Transplantation, Ministry of Public Health, School of Medicine, Zhejiang University, Hangzhou, 310003, PR China.*

[b] *College of Life Sciences, Huzhou University, Huzhou, 313000, PR China.*

[c] *Department of Medical Oncology; Sir Run Run Shaw Hospital; School of Medicine, Zhejiang University, Hangzhou, 310016, PR China.*

Corresponding Author: *Hangxiang Wang, The First Affiliated Hospital, School of Medicine, Zhejiang University; 79, Qingchun Road, Hangzhou, 310003, China. Phone: +86-571-88208173; Fax: +86-571-88208173; E-mail: wanghx@zju.edu.cn*

A. Experimental

^{1}H and ^{13}C NMR spectra were recorded on a Bruker Avance-400 (400 MHz) spectrometer at 400 MHz for ^{1}H and 100 MHz for ^{13}C. Chemical shifts (δ) are expressed in ppm downfield to TMS at $\delta = 0$ ppm and coupling constants (*J*) are expressed in Hz. Elemental analyses were performed with a Flash EA 1112 from ThermoFinnigan.

Synthesis of $[H_2L1](PF_6)_2$

3-(chloromethyl)-1-ethyl-5-methyl-pyrazole (2.0 g, 12.5 mmol) and 1,4-di(1-imidazolyl)benzene (1.05 g, 5.0 mmol) were dissolved in 10 mL of DMF and stirred at 100 °C overnight. The resulting white solid was collected by filtration and redissolved in 100 mL of water. The solution was filtered, followed by the subsequent addition of saturated aqueous NH_4PF_6 to afford a white precipitate, which was collected by filtration and dried. Yield: 2.58 g, 69%. Anal. Calcd for $C_{26}H_{32}F_{12}N_8P_2$: C, 41.83; H, 4.32; N, 15.01. Found: C, 41.86; H, 4.16; N, 15.31. ^{1}H NMR (400 MHz, DMSO-d_6): δ 10.00 (s, imidazolium acidic C2-H, 2H), 8.39, 8.03 (both s, imidazole CH, each 2H), 8.10 (s, benzene CH, 4H), 6.23 (s, pyrazole CH, 2H), 5.42 (s, CH_2, 4H), 4.05 (q, $J = 7.2$ Hz, CH_2CH_3, 4H), 2.27 (s, CH_3, 6H), 1.31 (t, $J = 7.2$ Hz, CH_2CH_3, 6H). ^{13}C NMR (100 MHz, DMSO-d_6): δ 143.7, 139.9, 136.2, 135.7, 124.0, 124.0, 121.9, 105.3, 47.4, 43.9, 15.6, 11.0.

Synthesis of $[H_3L2](PF_6)_3$

A solution of 1,3,5-tri(1-imidazolyl)benzene (1.38 g, 5.0 mmol) and 3-(chloromethyl)-1-methyl-5-methyl-pyrazole (2.88 g, 20 mmol) in 10 mL of DMF was stirred at 100 °C overnight. The resulting solid was collected by filtration and dissolved in 100 mL of water. Subsequent addition of saturated NH_4PF_6 aqueous to the solution afforded a white precipitate, which was collected by filtration and dried. Yield: 2.75 g, 53%. Anal. Calcd for $C_{33}H_{39}F_{18}N_{12}P_3$: C, 38.16; H, 3.78; N, 16.18. Found: C, 38.43; H, 3.91; N, 16.26. ^{1}H NMR (400 MHz, DMSO-d_6): δ 9.95 (s, imidazolium acidic C2-H, 3H), 8.53 (s, benzene CH, 3H), 8.41, 8.16 (both s, imidazole CH, each 3H),

6.25 (s, pyrazole CH, 3H), 5.50 (s, CH_2, 6H), 3.73 (s, NCH_3, 9H), 2.27 (s, CH_3, 9H). ^{13}C NMR (100 MHz, DMSO-d_6): δ 143.3, 140.8, 136.7, 136.1, 124.7, 121.9, 117.0, 105.2, 47.6, 36.5, 11.1.

Synthesis of [HL3](PF_6)

3-(chloromethyl)-1-methyl-5-methyl-pyrazole (1.44 g, 10 mmol) and 3-(2-picolyl)-imidazole (1.6 g, 10 mmol) were mixed in 10 mL CH_3CN and refluxed overnight. The resulting solid was separated and dissolved in water, and then a saturated NH_4PF_6 aqueous solution was added dropwise. The resulting yellow precipitate was obtained as yellow solid after stirring overnight. Yield: 3.0 g, 73%. Anal. Calcd for $C_{15}H_{18}F_6N_5P$: C, 43.59; H, 4.39; N, 16.94. Found: C,43.16; H, 4.78; N, 16.18. ^{1}H NMR (400 MHz, DMSO-d_6): δ 9.33 (s, imidazolium acidic C2-H, 1H), 8.55 (d, J = 4.8 Hz, pyridine CH, 1H), 7.89 (t, J = 8.0 Hz, pyridine CH, 1H), 7.77, 7.76 (both s, imidazole CH, each 1H), 7.48 (d, J = 8.0 Hz, pyridine CH, 1H), 7.40 (t, J = 4.8 Hz, pyridine CH, 1H), 6.12 (s, pyrazole CH, 1H), 5.58 (s, CH_2, 2H), 5.36 (s, CH_2, 2H), 3.75 (s, CH_3, 3H), 2.25 (s, CH_3, 3H). ^{13}C NMR (100 MHz, DMSO-d_6): δ 153.9, 159.9, 144.0, 139.7, 137.9, 137.2, 124.0, 123.7, 123.0, 122.9, 105.0, 53.5, 46.7, 43.7, 10.8.

Synthesis of [H_3L4](PF_6)$_3$

A solution of 1,3,5-tri(1-imidazolyl)benzene (1.38 g, 5.0 mmol) and 2-(chloromethyl)pyridine (2.5 g, 20 mmol) was stirred at 100 °C in 10 mL of DMF overnight. The resulting solid was dissolved in water. Subsequent addition of saturated NH_4PF_6 aqueous to the solution afforded a white precipitate. Yield: 3.16 g, 64%. Anal. Calcd for $C_{33}H_{30}F_{18}N_9P_3$: C, 40.14; H, 3.06; N, 12.77. Found: C, 40.23; H, 3.11; N, 12.65. ^{1}H NMR (400 MHz, DMSO-d_6): δ 10.07 (s, imidazolium acidic C2-H, 3H), 8.59 (s, pyridine CH + benzene CH, 6H), 8.48, 8.21 (both s, imidazole CH, each 3H), 7.96 (t, J = 8.0 Hz, pyridine CH, 3H), 7.65 (d, J = 8.0 Hz, pyridine CH, 3H), 7.46 (t, J = 7.2 Hz, pyridine CH, 3H), 5.77 (s, CH_2, 6H). ^{13}C NMR (100 MHz, DMSO-d_6): δ 153.2, 150.1, 138.1, 137.0, 136.7, 125.3, 124.4, 123.3, 121.7, 117.0, 54.2.

Synthesis of $[Ag_4(L1)_2](PF_6)_4]$, (1)

A mixture of $HL1(PF_6)$ (373 mg, 0.5 mmol) and Ag_2O (120 mg, 0.5 mmol) in 10 mL CH_3CN was stirred at 50°C for 6 h. Then, the mixture was filtered through Celite and all volatiles were evaporated under reduced pressure. The residue was dissolved in CH_3CN and crystallized by slow diffusion of Et_2O into the CH_3CN solution to give **1** as a colorless solid. Yield: 220 mg, 46%. Anal. Calcd for $C_{52}H_{60}Ag_4F_{24}N_{16}P_4$: C, 32.52; H, 3.15; N, 11.67. Found: C, 32.88; H, 3.16; N, 11.83. ^{1}H NMR (400 MHz, DMSO-d_6): δ 7.95, 7.90 (both s, imidazole CH, each 4H), 7.69 (s, benzene CH, 8H), 6.51 (s, pyrazole CH, 4H), 5.63 (s, CH_2, 8H), 4.21 (s, CH_2CH$_3$, 8H), 2.35 (s, CH_3, 12H), 1.20 (s, CH_2CH_3, 12H). ^{13}C NMR (100 MHz, DMSO-d_6): δ 182.9(Ag-C), 163.6, 160.3, 159.4, 130.7, 127.7, 127.0, 119.7, 37.8, 37.0, 4.7, 4.2.

Synthesis of $[Ag_6(L2)_2(CH_3CN)_3](PF_6)_6]$, (2)

Similar procedure as for complex **1**, silver-NHC complex **2** was obtained as colorless solid, 277 mg, 39%. Anal. Calcd for $C_{72}H_{81}Ag_6F_{36}N_{27}P_6$: C, 30.43; H, 2.87; N, 13.31. Found: C, 30.58; H, 2.66; N, 13.38. ^{1}H NMR (400 MHz, DMSO-d_6): δ 7.95, 7.91 (both s, imidazole CH, each 6H), 7.67 (s, benzene CH, 6H), 6.52 (s, pyrazole CH, 6H), 5.63 (s, CH_2, 12H), 4.21 (s, NCH_3, 18H), 2.34 (s, CH_3, 18H), 2.08 (s, CH_3CN, 9H). ^{13}C NMR (100 MHz, DMSO-d_6): δ 178.6 (Ag-C), 147.7, 142.6, 139.7, 125.0, 123.9, 124.3, 118.5, 107.0, 48.9, 45.2, 11.3, 1.5.

Synthesis of $[Ag_3(L4)_3](PF_6)_3]$, (3)

Similar procedure as for complex **1**, silver-NHC complex **3** was obtained as colorless solid, 163 mg, 63%. Anal. Calcd for $C_{45}H_{51}Ag_3F_{18}N_{15}P_3$: C, 34.64; H, 3.29; N, 13.46. Found: C, 34.91; H, 3.04; N, 13.83. ^{1}H NMR (400 MHz, DMSO-d_6): δ 8.04 (s, pyridine CH, 3H), 7.87-7.76 (m, pyridine CH, 9H), 7.39, 7.08 (both s, imidazole CH, each 3H), 6.28 (s, pyrazole CH, 3H), 5.58-5.09 (s, methylene, 12H), 3.10, 2.90 (s, CH_3, 9H), 2.22 (s, CH_3, 9H). ^{13}C NMR (100

MHz, DMSO-d_6): δ 174.3 (Ag-C), 153.9, 149.3, 146.9, 141.2, 140.1, 126.1, 125.6, 125.3, 125.2, 106.2, 65.4, 55.6, 47.9, 43.6, 11.0.

Synthesis of $[Ag_6(L3)_2(CH_3CN)_3](PF_6)_6]$, (4)

Similar procedure as for complex **1**, silver-NHC complex **4** was obtained as colorless solid, 282 mg, 41%. Anal. Calcd for $C_{72}H_{63}Ag_6F_{36}N_{21}P_6$: C, 31.57; H, 2.32; N, 10.74. Found: C, 31.50; H, 2.29; N, 10.78. ^{1}H NMR (400 MHz, DMSO-d_6): δ 8.75 (d, J = 6.4 Hz, pyridine CH, 6H), 8.02 (t, J = 8.0 Hz, pyridine CH, 6H), 7.93 (s, benzene CH, 6H), 7.83, 7.81 (both s, imidazole CH, each 6H), 7.64 (d, J = 8.0 Hz, pyridine CH, 6H), 7.59 (t, J = 6.4 Hz, pyridine CH, 6H), 5.71 (s, CH_2, 12H), 2.07 (s, CH_3CN, 9H). ^{13}C NMR (100 MHz, DMSO-d_6): δ 179.1(Ag-C), 155.2, 151.8, 140.8, 139.7, 125.0, 124.9, 124.2, 123.2, 118.6, 57.2, 1.5.

X-ray diffraction analysis

Single-crystal X-ray diffraction data were collected at 298(2) K on a Siemens Smart-CCD area-detector diffractometer with a Mo-Kα radiation (λ = 0.71073 Å) by using a ω-2θ scan mode. Unit-cell dimensions were obtained with least-squares refinement. Hydrogen atom positions for all of the structures were calculated and allowed to ride on their respective C atoms with C–H distances of 0.93–0.97 Å and U_{iso}(H) = –1.2–1.5U_{eq}(C). CCDC 1958763-1958766 contain the supplementary crystallographic data for this paper. These data can be obtained free of charge from The Cambridge Crystallographic Data Centre.

B. Materials and methods

***In vitro* Cytotoxicity using an MTT Assay**

The *in vitro* cytotoxicity of the silver-NHC complexes and cisplatin were measured by an MTT (3-(4,5-dimethylthiazol-2-yl)-2,5-diphenyltetrazolium bromide) assay. The cells were plated in 96-well plates (4000-5000 cells per well) and incubated at 37 °C overnight. The cells were supplemented with a serial dilution of silver-NHC complexes and cisplatin and then incubated at 37°C. Following exposure, 30 μL MTT solution (5 mg/mL in PBS) was added

to each well. The MTT solution was removed from the wells after 4 h and the purple MTT-formazan crystals were then dissolved by the addition of DMSO (100 μL). The absorbance in each well was measured at 490 nm using a microplate reader (Multiskan FC, Thermo Scientific, American).

Cell Proliferation as Determined by EdU Incorporation

LoVo cells were plated in 48-well plates (2×10^4 cells per well) and incubated at 37 °C for 24 h. Silver-NHC complexes **1-4** and cisplatin (2 and 4 μM) were added to the cells and then incubated for 48 h at 37 °C. To quantify the synthesized DNA, we used a Click-iT® EdU Alexa Fluor® 488 Assay Kit (Invitrogen) according to the manufacturer's protocol. At the end of the drug exposure, EdU (5-ethynyl-2'-deoxyuridine) was added to each well, and the cells were further incubated for 2 h at 37 °C. The cells were washed with PBS and fixed for 15 min at room temperature by the addition of 4% formaldehyde. After incubating with 0.5% Triton X-100 for 10 min, azide-labeled Alexa Fluor® 488 was added and incubated for 30 min in the dark. The nuclei were stained with Hoechst 33342 (Invitrogen) for 15 min and then the cells were imaged by fluorescence microscopy (Olympus, IX72, Japan). Finally, $n \geq 5$ regions with 1500-2000 total cells were counted to assess the presence of cell proliferation.

AO/EB and Trypan Blue Staining

LoVo cells were seeded in a glass-bottom dish (18×18 mm) at a density of 2×10^5 cells and cultured for 24 h. After treatment with complex **2** (0, 2 and 4 μM) or cisplatin (4 μM) for 6 h, the cells were washed with PBS, fixed in 4% chilled paraformaldehyde for 20 min, and then washed twice with PBS. For trypan blue staining, the cells were mixed with 0.1% TB for 5 min and washed with PBS. Blue and red fluorescence was imaged under a fluorescence microscope (Olympus, IX72). For AO/EB staining, the cells were then stained through the addition of 1 mL AO/EB mix (100 μg/mL AO and 100 μg/mL EB

in PBS). After 5 min of incubation, the cells were washed twice with PBS and visualized under a fluorescence microscope (Olympus, IX72, Japan).

Immunofluorescence Staining

LoVo cells were seeded in a glass-bottom dish (5×10^4 cells/well) and cultured for 24 h. The cells were treated with complex **2** (0, 2 and 4 μM) for 6 h. After incubation, the cells were washed three times of PBS and fixed with 4% paraformaldehyde for 30 min at room temperature. The cells were then permeated with 0.5% Triton X-100 in PBS for 1.5 h and blocked with goat serum for 1 h at RT. The cells were subsequently immunostained with α-tubulin antibody for 1 h, washed with PBS, and incubated with Alexa Fluor 555-labeled secondary antibody for 1 h. After a brief washing, F-actin was stained with Alexa Fluor 488-phalloidin for 40 min at RT, followed by nuclei staining with DAPI for 15 min. Finally, the cells were imaged by a Nikon fluorescence microscope (Nikon A1R, Japan).

Western Blot Analysis

LoVo cells were recovered following treatment with complex **2** (2 and 4 μM) and cisplatin (4 and 8 μM) and lysed in RIPA Lysis Buffer (Beyotime)-containing protease inhibitor phenylmethanesulfonyl fluoride (PMSF). A bicinchoninic acid protein assay was used to determine the protein concentration. Samples with equivalent amounts of protein were separated on 10% SDS-PAGE gels and then transferred to PVDF membranes. After incubation with specific antibodies, including cleaved PARP, cleaved Caspase 3 and 9 (Cell Signaling technology), HRP-linked secondary antibodies were added and the bands were visualized using the chemiluminescent substrate on Biorad .

Determination of Reactive Oxygen Species (ROS)

The generation of ROS in silver complex 2-treated cells was determined by 2,7-dichlorofluoresceindiacetate (DCFH-DA) staining. For this assay, LoVo cells were seeded in a 6-well plate (2×10^5 cells/well) and were grown for 24 h. After

24 h of growth, the cells were treated with 2 and 4 μM of silver complex **2** for 3 h, harvested, and washed twice with PBS. Finally, the cells were resuspended in 1 mL of 1640 solution with 5 μM DCFH-DA and incubated for 30 min at 37 °C. After incubation, the samples were washed with 1640 solution and analyzed for DCF fluorescence in a flow cytometer (Cytomic FC 500MCL, BECKMAN COULTER) at an excitation wavelength of 488 nm and an emission wavelength of 525 nm. The fluorescence data were recorded and analyzed with the CytExpert software with 1×10^4 cells in each sample. ROS generation was expressed in terms of the percentage of cells with DCF (green) fluorescence. A parallel batch of treated cells was stained with DCFH-DA and visualized under a fluorescence microscope (Olympus, IX72, Japan).

Determination of Mitochondrial Membrane Potential

LoVo cells (2×10^5 cells/well in a 6-well plate) grown for 24 h were treated with silver-NHC complex **2** (2 and 4 μM) for 6 h and then incubated with 5 μM of 5,5,6,6-tetrachloro-1,1,3,3-tetraethylbenzimidazolylcarbocyanine iodide (JC-1; Sigma-Aldrich, USA) for 30 min in a CO_2 incubator. After incubation, the cells were washed twice with prewarmed PBS, harvested, and analyzed with a flow cytometer (Cytoflex S, Beckman, American). The JC-1 fluorescence data were recorded and analyzed with the CytExpert software. A parallel batch of treated cells was stained with JC-1 and washed with PBS before visualization under a fluorescence microscope (Olympus, IX72, Japan).

Co-assembly of Silver-NHC with DSPE-PEG_{2k}

Silver-NHCs **1**, **2**, **3** or **4** were first blended with DSPE-PEG_{2k} in DMSO at pre-determined various weight ratios while maintaining the drug concentration at 40 mg/mL. Thereafter, the mixture (100 μL) was rapidly injected into DI water (1 mL) under ultrasonication. Prior to further use, the drug concentration was determined by UV detection (Shimadzu UV-2700, Japan).

Characterization of Particle Size by Dynamic Light Scattering (DLS)

The hydrodynamic diameters of silver-NHC-formulated nanoparticles **1**-NPs, **2**-NPs, and **4**-NPs were measured by DLS on a Malvern Nano-ZS90 instrument at 25°C; each sample was tested three times.(Malvern Nano-ZS90, U.K.)

Particle Morphology Study by Transmission Electron Microscopy (TEM)

To characterize the morphologies of the silver-NHC-formulated nanoparticles, TEM analysis was performed on a TECNAL 10 instrument (Philips) at an acceleration voltage of 80 kV. A droplet of silver-NHC-formulated nanoparticles at an appropriate concentration was placed on a 400-mesh copper grid coated with carbon. Positive staining was performed with a 2 wt % aqueous uranyl acetate solution after the carbon surface was completely dry. The morphology of the nanoparticles was also observed with a Hitachi SU-8010 Cold Field Emission Scanning Electron Microscope.(Hitachi SU-8010 SEM, Japan)

Toxicity Studies on the Silver-NHC-loaded Nanoparticles

The toxicity of the silver-NHC-loaded nanoparticles **1**-NPs, **2**-NPs, and **4**-NPs and cisplatin was investigated in ICR mice. A total of 40 mice were randomly divided into eight groups. In seven groups, the drugs were administered through the tail vein in a single dose three times every 3 d; the remaining group was treated with PBS as a control. The body weights were recorded for evaluation of drug toxicity.

***In vivo* Antitumor Activity in the LoVo Cell-derived Xenograft Mouse Model using Silver-NHC-loaded Nanoparticles**

Balb/c nude mice bearing LoVo tumor xenografts were utilized for the evaluation of the *in vivo* antitumor efficacy. After the LoVo tumor reached ~50 mm^3 in volume after implantation, the animals were randomized into seven groups (n = 6 in each group). The mice were intravenously injected with the nanoparticles and cisplatin (1.25, 2.5, or 5 mg/kg) three successive times on days 0, 3, and 6. Saline was intravenously injected as a control. The tumor growth and body weight were monitored and recorded every three days. The

length (L) and width (W) of the tumors were measured with calipers, and the tumor volume was calculated using the following formula: $V = L \times W^2/2$, where W was smaller than L.

Statistical Analysis

All of the quantitative data are presented as the means ± SD. The statistical significance between the measurements was assessed using Student's t test. A p-value less than 0.05 was considered statistically significant, whereas a p-value less than 0.01 was considered highly significant.

C. Table S1. X-ray crystallographic data of complexes 1-3 and 4s.

	1	**2**	**3**	**4s**
formula	$C_{60}H_{72}Ag_4F_{30}N_{20}P_4$	$C_{164}H_{192}Ag_{12}F_{72}N_{64}P_{12}$	$C_{53}H_{67}Ag_3F_{18}N_{17}O_1P_3$	$C_{75}H_{75}Ag_6F_{36}N_{21}O_3P_6$
Fw.	2198.74	6093.90	1731.73	2835.60
crystal system	Monoclinic	Monoclinic	Monoclinic	Monoclinic

space group	C2/c	C2/c	C2/c	P2(1)
a/Å	25.685(15)	41.409(4)	18.8950(9)	13.876(8)
b/Å	21.237(13)	18.5246(18)	23.5495(9)	25.304(14)
c/Å	19.52(2)	37.892(4)	15.6257(7)	15.283(8)
β/deg	90	90	90	90
V/Å^3	8806(12)	24607(4)	6939.7(5)	5163(5)
Z	4	4	4	2
D_{calcd}, Mg/m^3	1.658	1.645	1.657	1.824
Refls collected	21666	61593	13612	26058
Independent reflections, R_{int}	7747, 0.0332	21625, 0.0401	6096, 0.0409	15592, 0.0515
Goodness-of-fit on F^2	1.064	1.096	1.018	1.042
$R1$, $wR2$ [$I > 2\sigma(I)$]	0.0761, 0.2115	0.0851, 0.2198	0.0503, 0.1216	0.0636, 0.1558
$R1$, $wR2$ (all data)	0.0925, 0.2355	0.1165, 0.2415	0.0821, 0.1491	0.0868, 0.1787
Largest diff. peak and hole (e. Å^{-3})	4.565 and -1.909	2.002 and -1.659	1.091 and -0.514	1.260 and -0.995

D. The Crystal Structures of Complex 4s

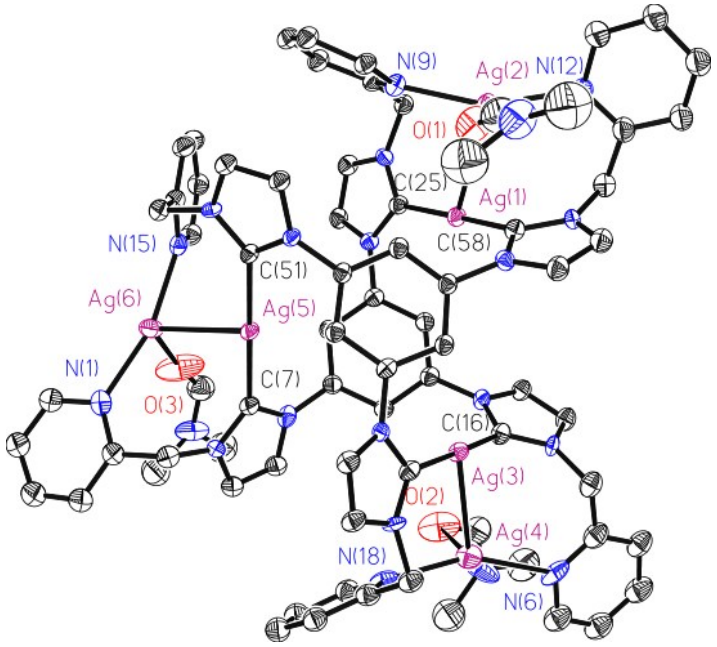

Figure S1. ORTEP view of **4s**. Thermal ellipsoids are 30 % probability level. All hydrogen atoms have been omitted for clarity.

E. Table S2. Selected bond distances (Å) and angles (deg) for silver-NHC complexes **1-3** and **4S**.

$[Ag_4(L1)_2](PF_6)_4$ (**1**)

Ag(1)-C(19)	2.111(7)	C(19)-Ag(1)-C(4)	172.2(3)
Ag(1)-C(4)	2.124(7)	C(19)-Ag(1)-Ag(2)	81.52(19)
Ag(1)-Ag(2)	3.2598(19)	C(4)-Ag(1)-Ag(2)	104.7(2)
Ag(2)-N(7)	2.143(7)	N(7)-Ag(2)-N(3)	168.3(3)
Ag(2)-N(3)	2.145(7)	N(7)-Ag(2)-Ag(1)	106.56(18)
		N(3)-Ag(2)-Ag(1)	77.51(18)
		N(6)-C(19)-Ag(1)	128.9(5)
		N(5)-C(19)-Ag(1)	127.3(5)
		C(17)-C(18)-N(6)	108.6(8)

Symmetry transformations used to generate equivalent atoms: #1 -x, y, -z+1/2, #2 -x+1, y, -z+1/2

$[Ag_6(L2)_2(CH_3CN)_3](PF_6)_6$ (**2**)

Ag(1)-C(25)	2.073(9)	C(25)-Ag(1)-C(49)	179.5(3)

Ag(1)-C(49)	2.074(10)	C(25)-Ag(1)-Ag(5)	70.6(2)
Ag(1)-Ag(5)	2.9452(11)	C(49)-Ag(1)-Ag(5)	109.1(3)
Ag(2)-C(16)	2.063(8)	C(16)-Ag(2)-C(58)	177.6(3)
Ag(2)-C(58)	2.074(9)	C(16)-Ag(2)-Ag(4)	107.2(2)
Ag(2)-Ag(4)	2.8856(11)	C(58)-Ag(2)-Ag(4)	70.7(3)
Ag(3)-C(7)	2.103(9)	C(7)-Ag(3)-N(16)	164.8(3)
Ag(3)-N(16)	2.143(9)	C(7)-Ag(3)-Ag(6)	72.4(2)
Ag(3)-Ag(6)	2.8858(12)	N(16)-Ag(3)-Ag(6)	109.4(2)
Ag(4)-N(7)	2.179(8)	N(7)-Ag(4)-N(23)	134.6(3)
Ag(4)-N(23)	2.225(8)	N(7)-Ag(4)-N(27)	119.6(3)
Ag(4)-N(27)	2.347(9)	N(23)-Ag(4)-N(27)	95.8(3)
Ag(5)-N(19)	2.176(9)	N(7)-Ag(4)-Ag(2)	90.6(2)
Ag(5)-N(12)	2.213(9)	N(23)-Ag(4)-Ag(2)	103.0(2)
Ag(5)-N(26)	2.408(13)	N(27)-Ag(4)-Ag(2)	110.8(2)
Ag(6)-C(40)	2.102(10)	N(19)-Ag(5)-N(12)	140.2(3)
Ag(6)-N(3)	2.175(11)	N(19)-Ag(5)-N(26)	116.2(3)
Ag(6)-N(25)	2.511(11)	N(12)-Ag(5)-N(26)	92.9(4)
		N(19)-Ag(5)-Ag(1)	88.4(2)

Symmetry transformations used to generate equivalent atoms.

$[Ag_3(L3)_3](PF_6)_3$ (**3**)

Ag(1)-C(17)	2.267(7)	C(17)-Ag(1)-C(9)	165.1(2)
Ag(1)-C(9)	2.287(6)	C(17)-Ag(1)-N(7)	83.8(6)
Ag(1)-N(7)	2.350(15)	C(9)-Ag(1)-N(7)	106.2(6)
Ag(1)-N(4)	2.353(5)	C(17)-Ag(1)-N(4)	105.14(16)
Ag(1)-N(7A)	2.498(17)	C(9)-Ag(1)-N(4)	84.9(2)
Ag(1)-Ag(2)	2.7687(7)	N(7)-Ag(1)-N(4)	97.3(6)
Ag(1)-Ag(1)#2	2.7728(9)	C(17)-Ag(1)-N(7A)	89.5(6)
Ag(2)-C(9)#2	2.291(7)	C(9)-Ag(1)-N(7A)	99.4(6)
Ag(2)-C(9)	2.291(7)	N(7)-Ag(1)-N(7A)	8.4(12)
Ag(2)-N(1)	2.440(5)	N(4)-Ag(1)-N(7A)	101.9(7)
Ag(2)-N(1)#2	2.440(5)	C(17)-Ag(1)-Ag(2)	112.24(14)
Ag(2)-Ag(1)#2	2.7687(7)	C(9)-Ag(1)-Ag(2)	52.86(15)
		N(7)-Ag(1)-Ag(2)	132.4(6)
		C(9)-Ag(2)-N(1)	86.4(2)
		C(9)#2-Ag(2)-N(1)#2	86.4(2)
		N(1)-Ag(2)-N(1)#2	109.2(3)
		C(9)#2-Ag(2)-Ag(1)#2	52.71(14)
		C(9)-Ag(2)-Ag(1)#2	112.81(14)
		N(1)-Ag(2)-Ag(1)#2	124.69(13)
		N(1)#2-Ag(2)-Ag(1)#2	115.69(13)

		C(9)#2-Ag(2)-Ag(1)	112.81(14)
		C(9)-Ag(2)-Ag(1)	52.71(14)
		N(1)-Ag(2)-Ag(1)	115.69(13)
		N(1)#2-Ag(2)-Ag(1)	124.69(13)
		Ag(1)#2-Ag(2)-Ag(1)	60.10(2)

Symmetry transformations used to generate equivalent atoms: #1 -x,-y,-z; #2 -x,y,-z+1/2; #3 -x+1,y,-z+1/2

$[Ag_6(L4)_2(DMF)_3](PF_6)_6$ (**4S**)

Ag(3)-C(40)	2.070(12)	C(40)-Ag(3)-C(16)	177.2(5)
Ag(3)-C(16)	2.092(13)	C(40)-Ag(3)-Ag(4)	106.1(3)
Ag(3)-Ag(4)	2.8858(18)	C(16)-Ag(3)-Ag(4)	73.7(4)
Ag(1)-C(58)	2.061(14)	C(58)-Ag(1)-C(25)	178.2(5)
Ag(1)-C(25)	2.108(13)	C(58)-Ag(1)-Ag(2)	71.0(4)
Ag(1)-Ag(2)	2.9209(18)	C(25)-Ag(1)-Ag(2)	109.3(3)
Ag(5)-C(51)	2.067(12)	C(51)-Ag(5)-C(7)	179.4(5)
Ag(5)-C(7)	2.094(13)	C(51)-Ag(5)-Ag(6)	105.9(3)
Ag(5)-Ag(6)	2.8964(18)	C(7)-Ag(5)-Ag(6)	73.7(4)
Ag(6)-N(1)	2.159(13)	N(1)-Ag(6)-N(15)	163.4(4)
Ag(6)-N(15)	2.171(11)	N(1)-Ag(6)-O(3)	84.2(6)
Ag(6)-O(3)	2.566(12)	N(15)-Ag(6)-O(3)	97.4(5)
Ag(2)-N(9)	2.218(10)	N(1)-Ag(6)-Ag(5)	112.5(4)
Ag(2)-N(12)	2.227(11)	N(15)-Ag(6)-Ag(5)	82.8(3)
Ag(2)-O(1)	2.573(10)	O(3)-Ag(6)-Ag(5)	107.7(5)
Ag(4)-N(18)	2.200(13)	N(9)-Ag(2)-N(12)	158.5(4)
Ag(4)-N(6)	2.234(12)	N(9)-Ag(2)-O(1)	95.4(4)
Ag(4)-O(2)	2.560(12)	N(12)-Ag(2)-O(1)	93.5(4)
		N(9)-Ag(2)-Ag(1)	84.1(3)
		N(12)-Ag(2)-Ag(1)	113.6(3)
		O(1)-Ag(2)-Ag(1)	100.1(3)
		N(18)-Ag(4)-N(6)	155.4(5)
		N(18)-Ag(4)-O(2)	96.1(5)
		N(6)-Ag(4)-O(2)	91.0(5)

Symmetry transformations used to generate equivalent atoms.

F. ^{1}H and ^{13}C NMR Spectra

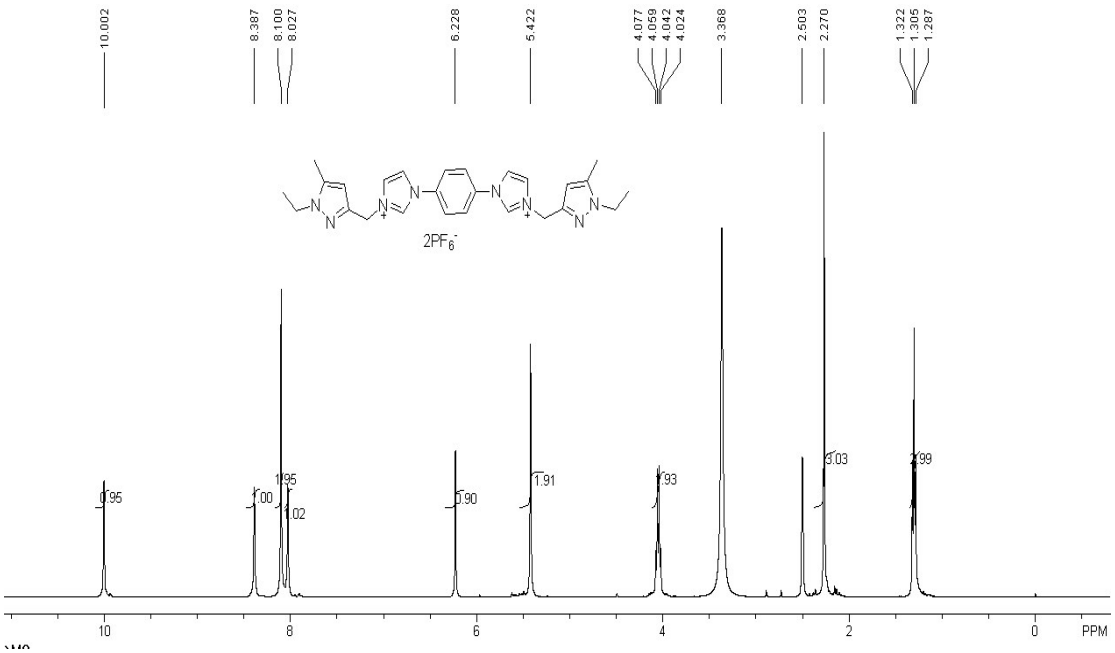

^{1}H NMR of $[H_2L1](PF_6)_2$

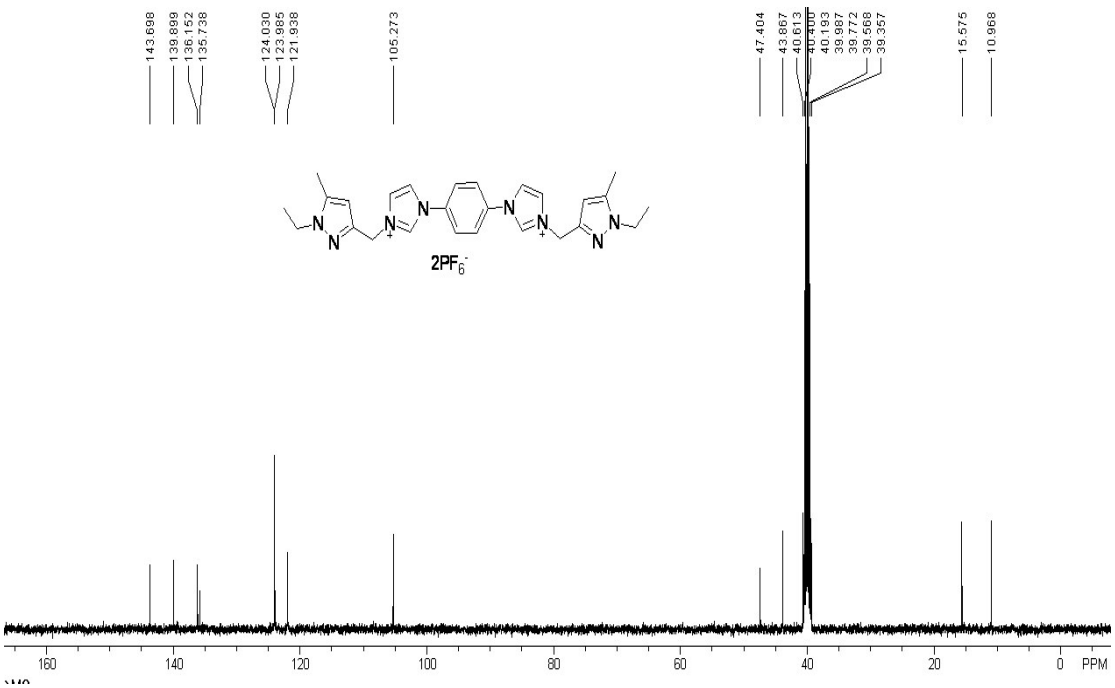

^{13}C NMR of $[H_2L1](PF_6)_2$

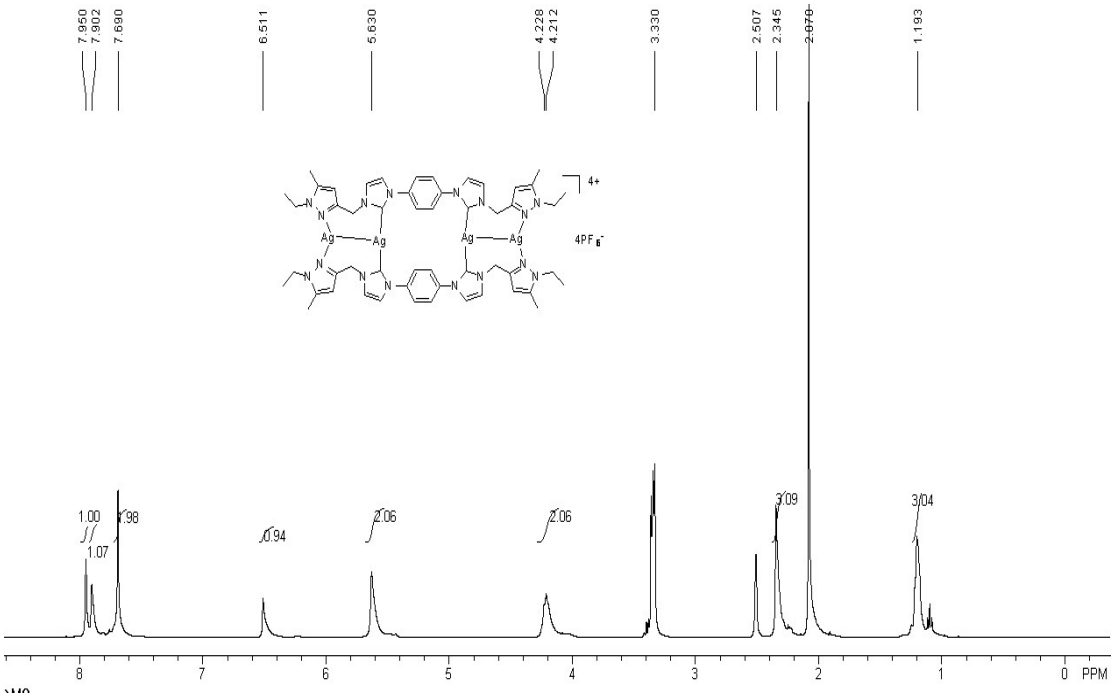

^{1}H NMR of $[Ag_4(L1)_2](PF_6)_4$ (**1**)

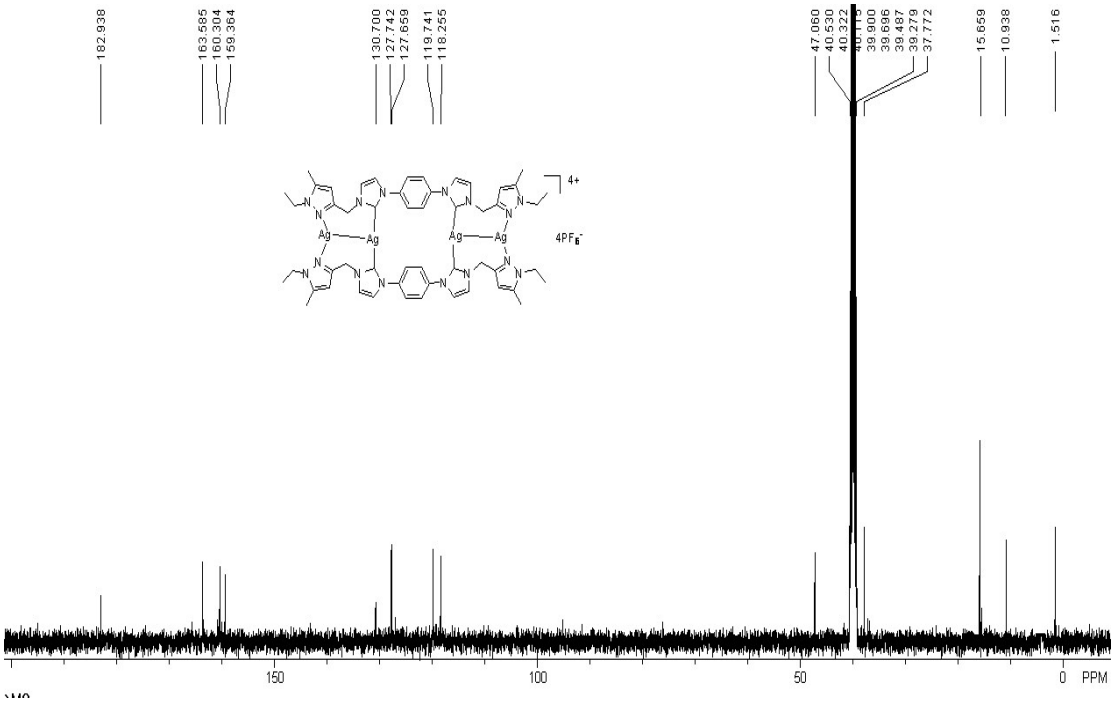

^{13}C NMR of $[Ag_4(L1)_2](PF_6)_4$ (**1**)

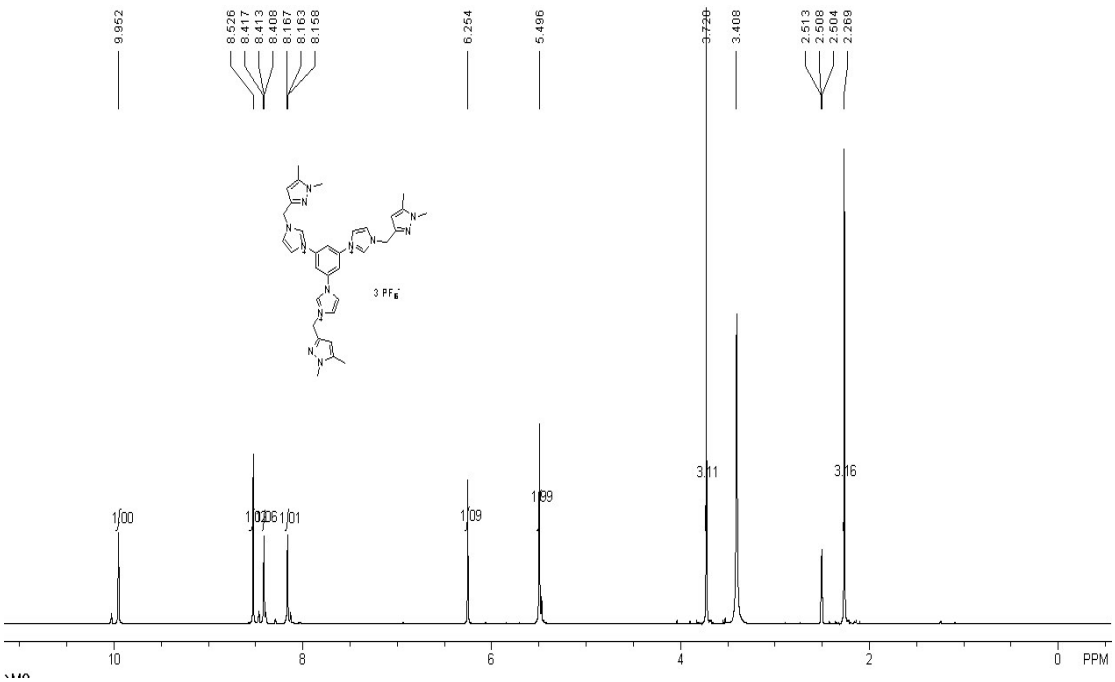

^{1}H NMR of $[H_3L2](PF_6)_3$

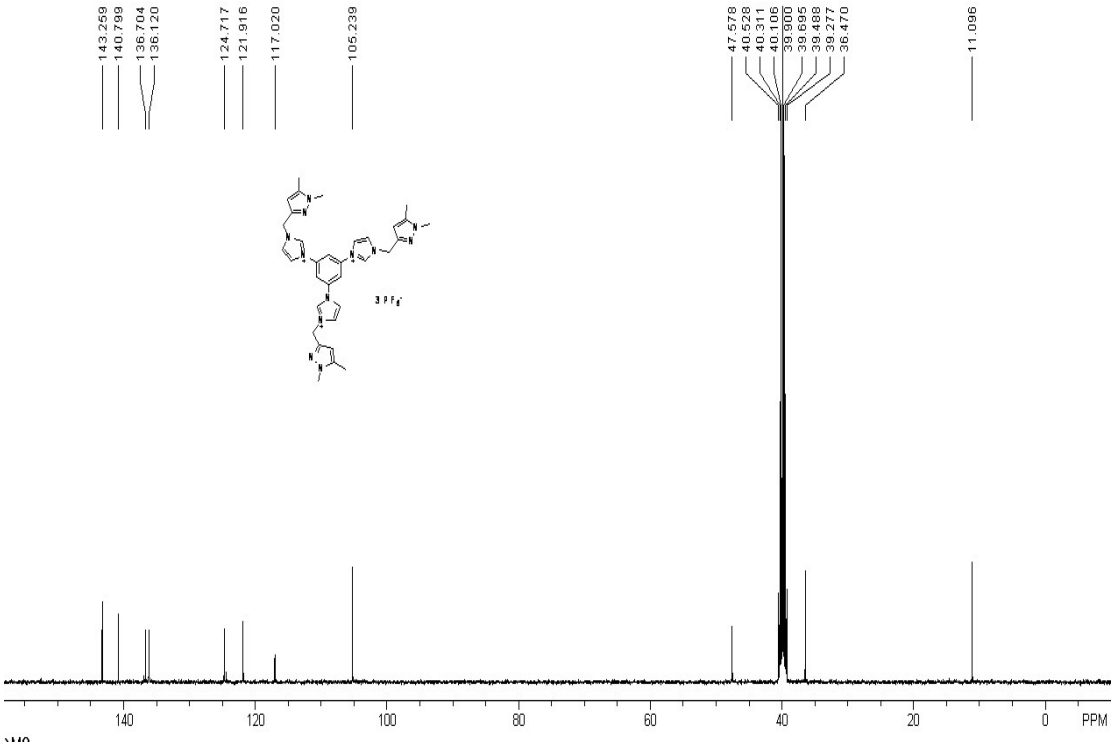

^{13}C NMR of $[H_3L2](PF_6)_3$

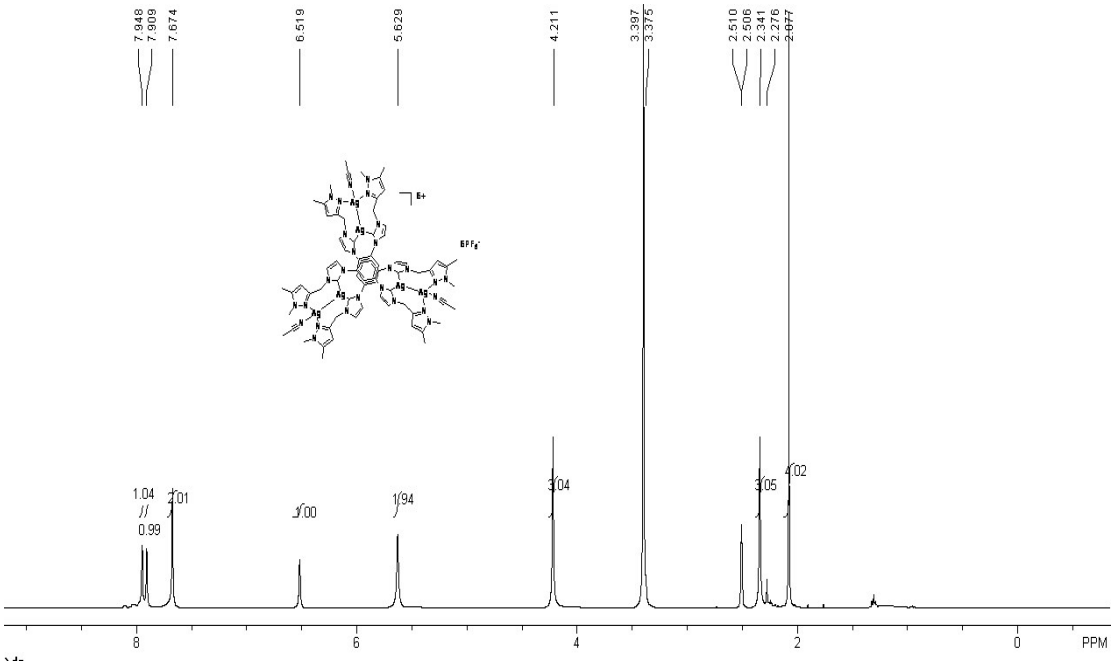

^{1}H NMR of $[Ag_6(L2)_2(CH_3CN)_3](PF_6)_6$ (**2**)

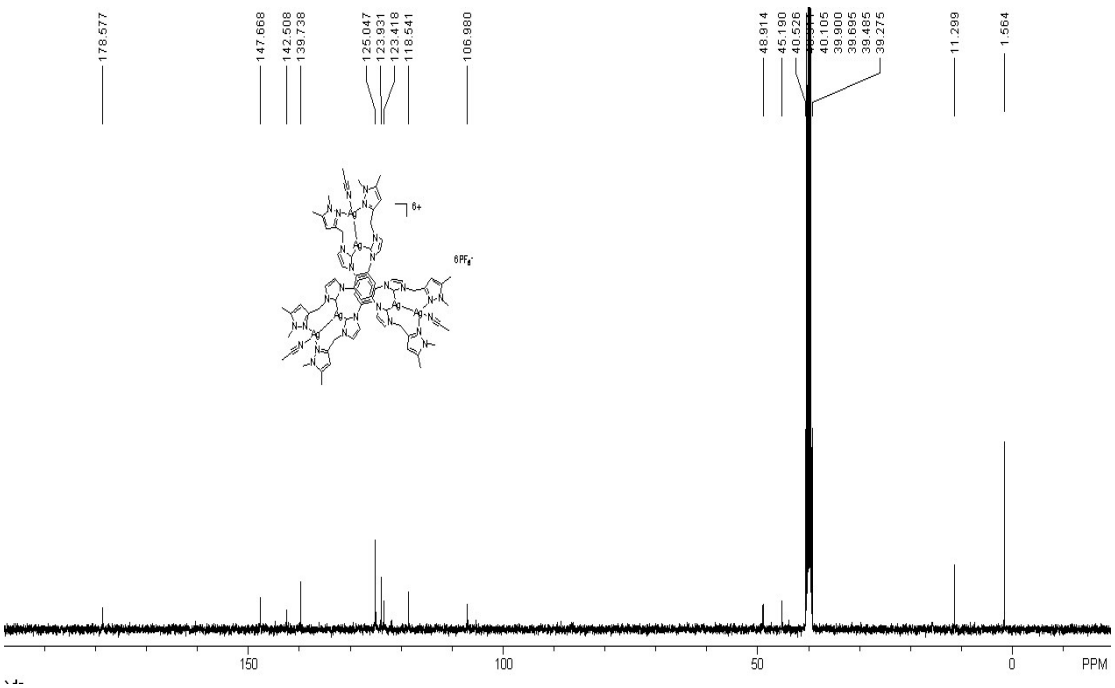

^{13}C NMR of $[Ag_6(L2)_2(CH_3CN)_3](PF_6)_6$ (**2**)

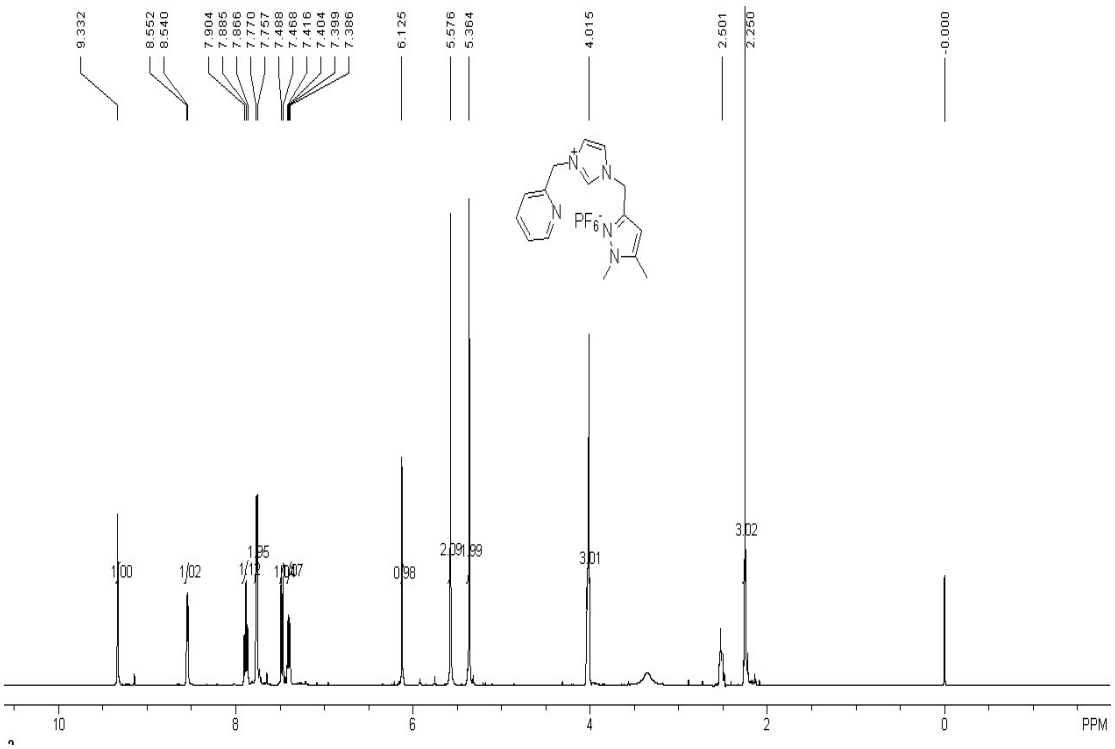

^{1}H NMR of [HL3](PF$_6$)

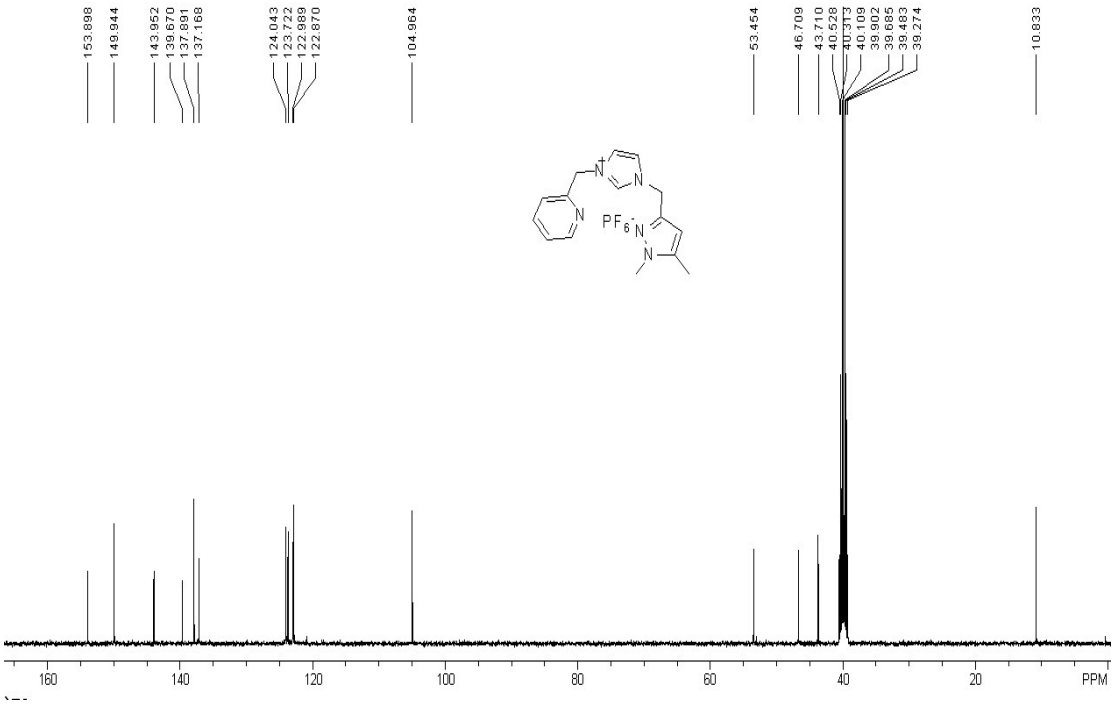

^{13}C NMR of [HL3](PF$_6$)

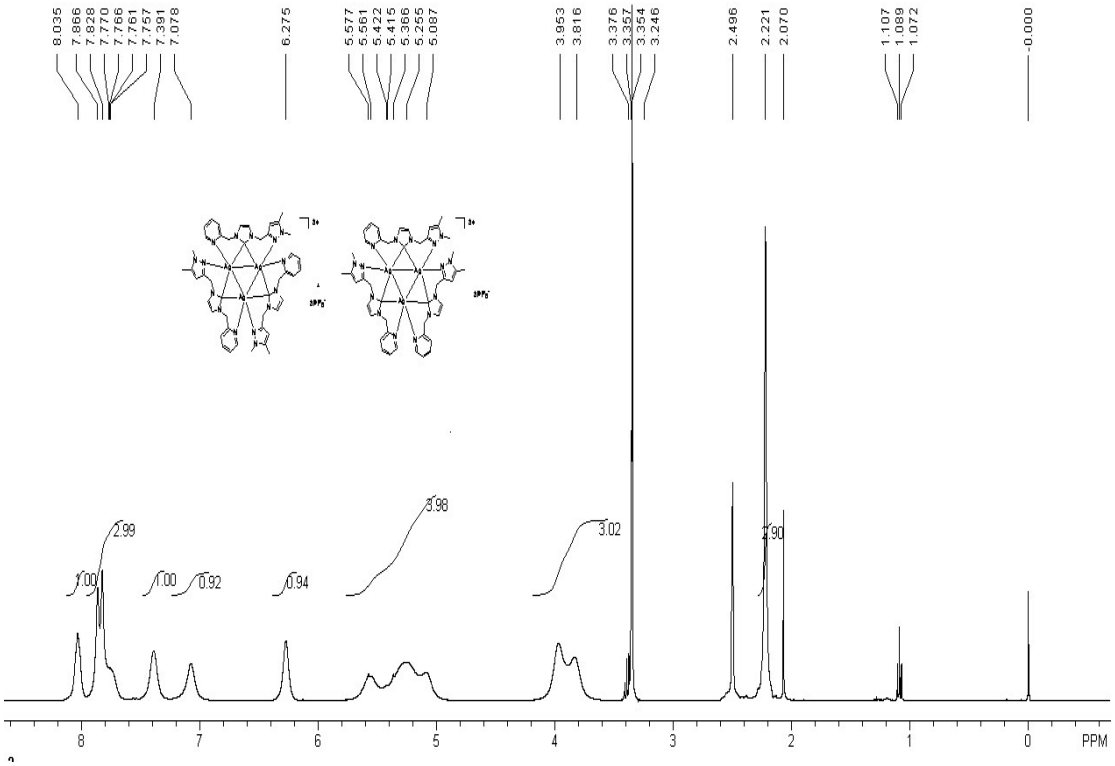

^{1}H NMR of $[Ag_3(L3)_3](PF_6)_3$ (**3**)

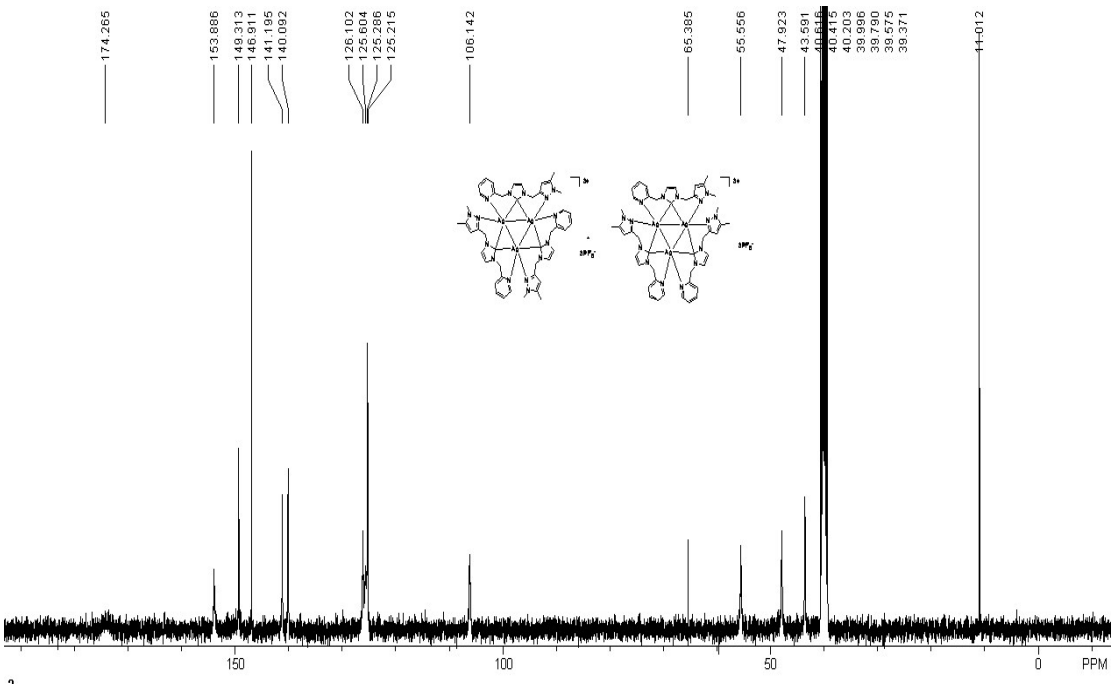

^{13}C NMR of $[Ag_3(L3)_3](PF_6)_3$ (**3**)

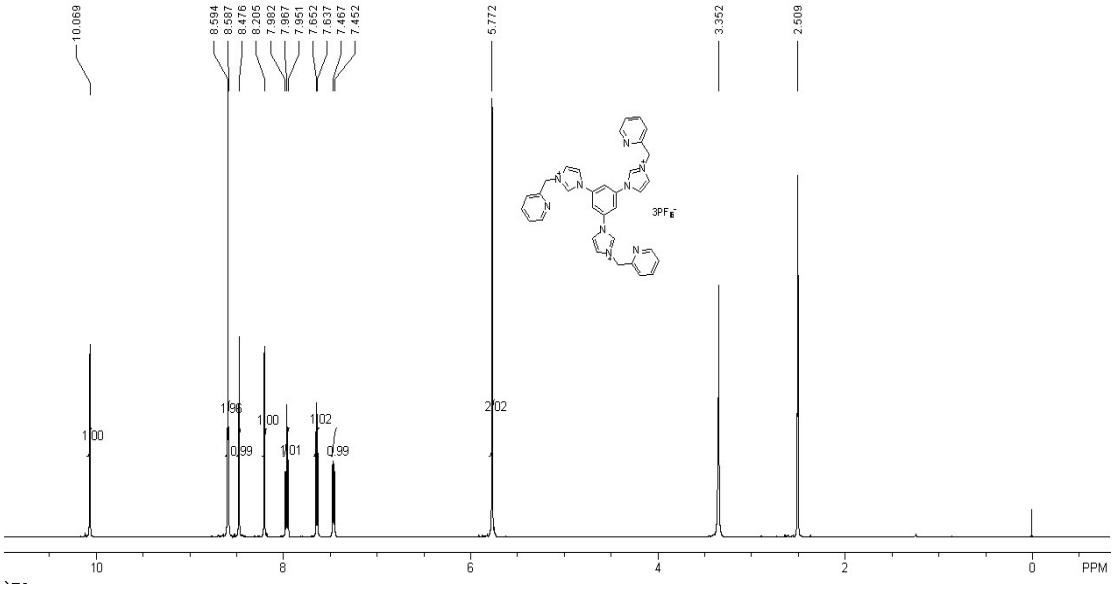

^{1}H NMR of $[H_3L4](PF_6)_3$

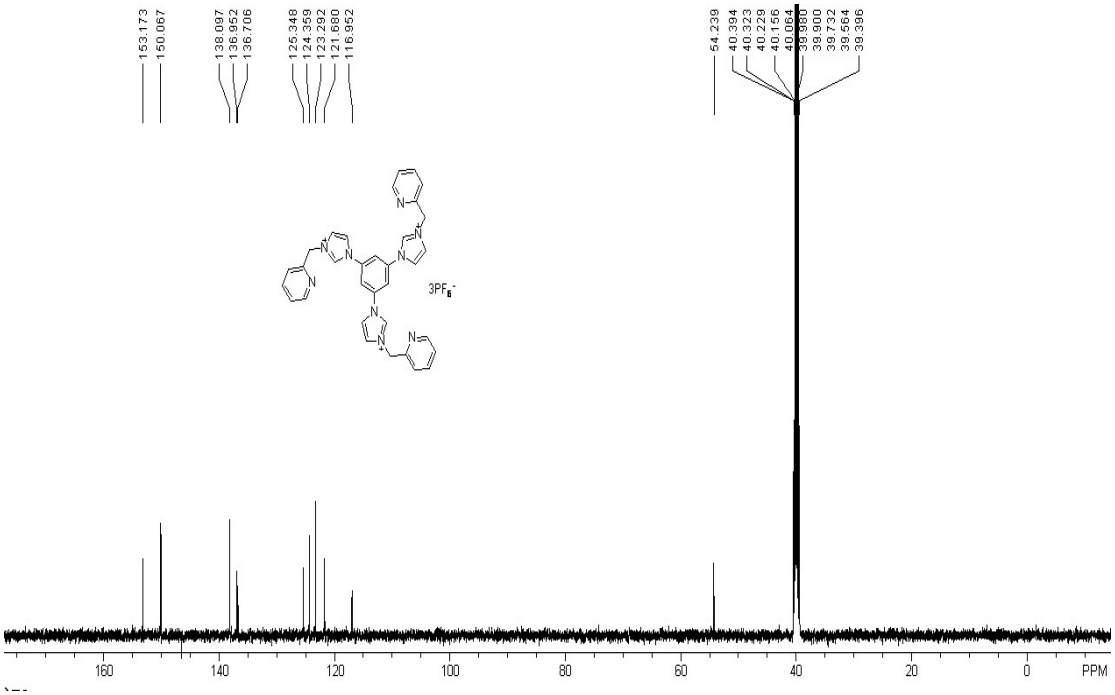

^{13}C NMR of $[H_3L4](PF_6)_3$

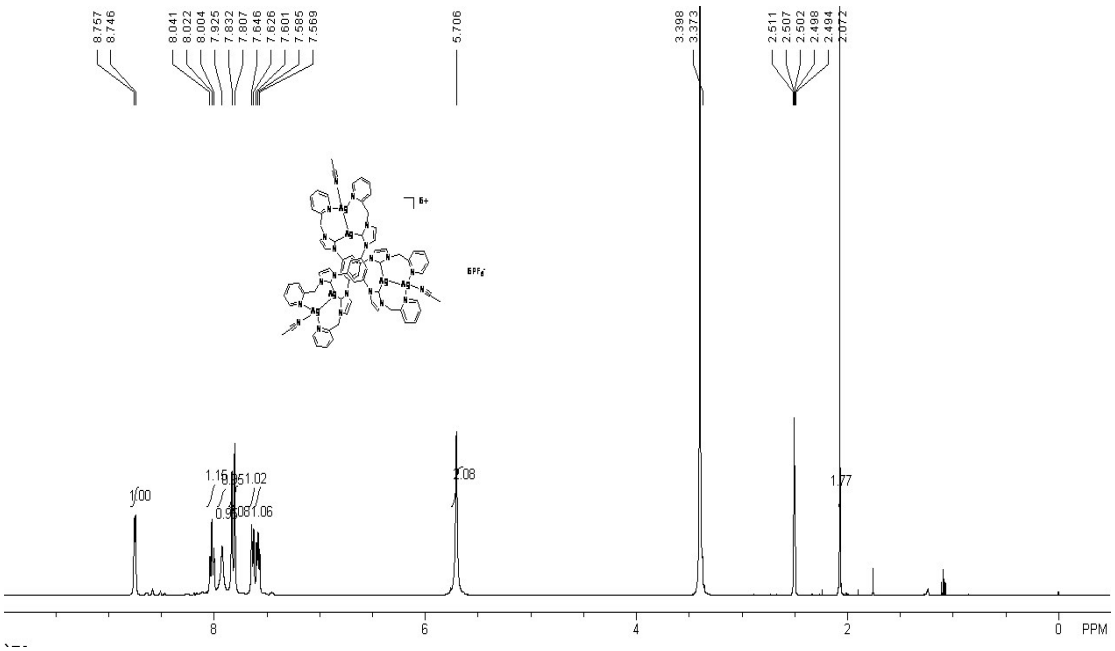

^{1}H NMR of $[Ag_6(L4)_2(CH_3CN)_3](PF_6)_6$ (**4**)

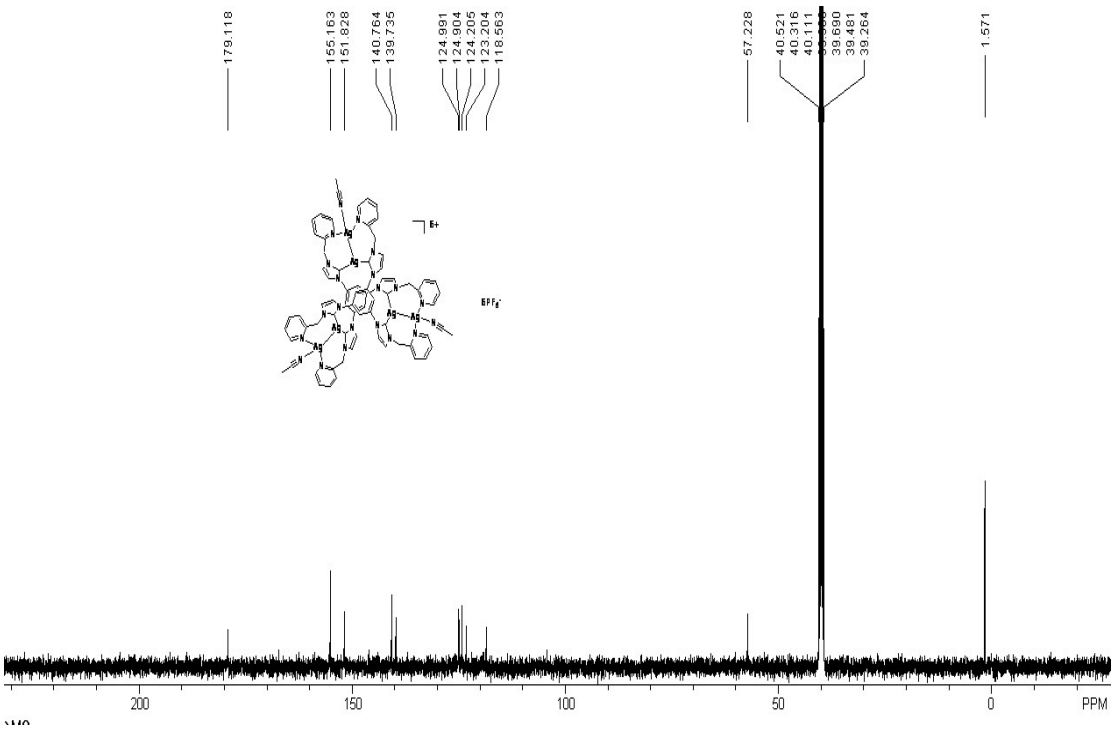

^{13}C NMR of $[Ag_6(L4)_2(CH_3CN)_3](PF_6)_6$ (**4**)